Infrared Photodissociation Spectroscopy of $Mg^+(CO_2)_n$ and $Mg^+(CO_2)_nAr$ Clusters

G. Gregoire, N. R. Brinkmann, D. van Heijnsbergen,† H. F. Schaefer, and M. A. Duncan*

Department of Chemistry, University of Georgia, Athens, Georgia 30602-2556

Received: June 24, 2002; In Final Form: October 22, 2002

$Mg^+(CO_2)_n$ and $Mg^+(CO_2)_nAr$ ion−molecule complexes are produced by laser vaporization in a pulsed-nozzle source and studied with mass-selected infrared photodissociation spectroscopy. Photodissociation of $Mg^+(CO_2)_n$ occurs by elimination of one or more intact CO_2 molecules, while $Mg^+(CO_2)_nAr$ species eliminate argon. Infrared resonance-enhanced photodissociation (IR-REPD) spectra are obtained by measuring the fragment yield versus energy near the asymmetric stretch vibration of CO_2 (2349 cm^{-1}). Structured vibrational bands are measured that are mostly blue shifted with respect to the vibration in the free molecule. In $Mg^+(CO_2)_n$ complexes, higher laser powers are required to achieve photodissociation, and the resonances are broad. In $Mg^+(CO_2)_nAr$ complexes, fragmentation is more efficient and the bands are sharper. For the smaller complexes $Mg^+(CO_2)_{n=1-3}$, the number of IR bands and their positions are in good agreement with theoretical predictions. The results provide strong evidence for a linear structure for Mg^+-CO_2, a bent configuration for $Mg^+(CO_2)_2$, and a trigonal pyramidal structure for $Mg^+(CO_2)_3$. Larger complexes have vibrational bands near the free-CO_2 asymmetric stretch, indicating the presence of CO_2 ligands not attached to the metal.

Introduction

Gas-phase metal ion chemistry provides detailed studies of metal−ligand interactions and metal ion solvation.[1−4] Many studies have focused on the energetics of bonding and on reaction mechanisms using conventional mass spectrometry methods.[5−10] However, spectroscopic studies to measure ion structures have been problematic. In recent years, electronic photodissociation spectroscopy has emerged as an effective approach to probe the electronic states of small metal ion complexes and in some cases the structures of these complexes have been determined.[11−23] Theory has investigated metal ion complexes,[24−31] but it has been difficult to compare theory and experiment directly. Electronic spectroscopy probes excited states that may be difficult to treat with theory. Ground-state spectroscopy is possible in principle through infrared photodissociation[32] or through ZEKE photoelectron spectroscopy[33,34] measurements. These methods have been applied widely to nonmetal complexes, but less so for metal-containing systems. Using new OPO infrared lasers, our group has recently begun an effort into the IR spectroscopy of metal ion complexes.[35,36] In the present report, we describe our measurements on $Mg^+(CO_2)_n$ and $Mg^+(CO_2)_nAr$ complexes.

Among the metal ion complexes studied previously with electronic spectroscopy, those with the group II metals have been a major focus because of their simple electronic structure.[13−21] These metal ions have one valence electron in an $ns^1(^2S)$ ground state, and there are strongly allowed ($^2P \leftarrow {}^2S$) electronic transitions at low energy. These ions are relatively unreactive (insertion chemistry is endothermic with many small molecules), and therefore electrostatic complexes form efficiently. Because the perturbation on the metal ion is not large, the strong atomic resonance line is preserved in metal ion complexes. Although there are shifts and multiplet splittings due to the details of ligand interactions, the spectra of complexes are often found close to the energy of the free ion resonance. Mg^+, Ca^+, and Sr^+ complexes of the form M^+-L_x have been studied with rare gas atoms and many small molecules using electronic photodissociation spectroscopy.[13−21] These studies yielded electronic state energies, excited state vibrational frequencies and bond energies for many complexes. Because magnesium ions have relatively few electrons, theory has examined the structures of various Mg^+L_n complexes and these results have been compared to experiments.[24] In the case of $Mg^+(CO_2)$, for example, experimental work in our group has found a sharp spectrum consistent with a linear Mg^+-OCO complex,[16b] in agreement with theory,[24b] and as expected for a charge−quadrupole binding interaction. A similar spectrum and a linear structure is found for $Ca^+(CO_2)$,[17] and transition metal ion complexes with CO_2 have also been found to form linear complexes.[12] However, larger $Mg^+(CO_2)_n$ complexes ($n>1$) have broad spectra without vibrational structure due to photoinduced reactions and predissociation.[16a,18b] These dynamics have also been seen for many metal ion complexes with multiple ligands. Consequently, sharp vibrational structure is often observed in the electronic spectra of monoligand complexes, but vibrational structure is almost never seen for any larger systems.[37] Infrared spectroscopy studies in the ground electronic state are not likely to cause photoinduced reactions, and even if the electronic structure changes because of reactions, IR measurements should still be possible. Therefore, we are pursuing IR measurements on many of these same group II metal ion complexes. We examine $Mg^+(CO_2)_n$ systems first because of the previous electronic spectroscopy[16] and theory[24b] already performed on these complexes.

Infrared spectroscopy is a standard method for inorganic or organometallic complexes in the condensed phase,[38] but IR measurements on metal ion complexes suffer from low sample density and the required intense IR light sources are not generally available. However, progress with IR optical parametric oscillator (OPO) systems has stimulated a new generation

* Corresponding author. E-mail: maduncan@uga.edu.
† Institute for Plasmaphysics Rijnhuizen, Edisonbaan 14, 3439 MN, Nieuwegein, The Netherlands.

10.1021/jp026373z CCC: $25.00
Published on Web 12/14/2002

of IR measurements on both neutral complexes and ion−molecule complexes. Lisy and co-workers were the first to direct this technology to metal systems in their studies on alkali cation complexes.[32] In recent work, our group has combined IR−OPO lasers with clusters produced by laser vaporization to obtain the first IR spectra of transition metal complexes in the gas phase.[35] Complexes of the form $Fe^+(CO_2)_n$ and $Fe^+(CO_2)_nAr_m$ were studied near the CO_2 asymmetric stretch (ν_3) region (2349 cm^{-1} in the isolated CO_2 molecule). These studies provided structures for the small complexes and they provided the first evidence for the formation of solvation spheres in these systems. In the present paper, we present the corresponding infrared photodissociation spectroscopy of $Mg^+(CO_2)_n$ and $Mg^+(CO_2)_n$-Ar complexes and compare the results to theoretical calculations of structures and vibrational frequencies.

Experimental Section

$Mg^+(CO_2)_n$ and $Mg^+(CO_2)_nAr$ clusters are produced by laser vaporization in a pulsed nozzle cluster source. The third harmonic (355 nm) of a Spectra Physics Nd:YAG laser (Quanta Ray INDI 30) is used to vaporize a rotating magnesium rod. Clusters are formed in a supersonic expansion of pure CO_2, or with a few percent of CO_2 seeded in argon, using a General Valve with a 1 mm nozzle at backing pressure of 40 psig. The operation of the molecular beam machine and mass spectrometer has been described previously.[18] The ions are skimmed from the source chamber into the mass spectrometer chamber and extracted from the molecular beam by pulsed acceleration voltages. They are then mass selected with pulsed deflection plates before reaching the reflectron region, where the infrared laser beam intersects them at the turning point in the reflectron field to induce their photodissociation. The laser beam is focused or not, depending on the intensity required and the fragmentation yield. Both parent and fragment ions drift through a second flight tube where they are mass analyzed by their time-of-flight. The output of the electron multiplier tube (EMT) detector is recorded with a digital oscilloscope (LeCroy Waverunner model LT-342) and transferred to a PC via an IEEE−488 interface. Infrared resonance enhanced photodissociation (IR-REPD) spectra are recorded by monitoring the intensity of fragment ion(s) as a function of the wavelength.

An IR OPO/OPA laser (Laser Vision) pumped by a Continuum 9010 Nd:YAG laser is used to photodissociate the clusters. This system has two 532-nm-pumped KTP crystals in the grating tuned oscillator section and four KTA crystals in the amplifier section. The signal output from the oscillator is combined with residual 1064 nm in the amplifier, and difference frequency generation here provides the tunable near-IR output from 2.2 to 4.9 μm (4500 to 2050 cm^{-1}). Pulse energies ranging from 15 to 1 mJ, respectively, and the line width is on the order of 0.3 cm^{-1}. A typical spectrum is obtained with a 1.2 cm^{-1} scan step and averaged over 250 laser shots. In so-called "low power" experiments, the unfocused laser is used, which has a pulse energy of 1−3 mJ/pulse near 2350 cm^{-1}. In so-called "high" laser power conditions, this light is focused with a 25 cm focal length lens.

Density functional theory (DFT) quantum chemical computations were performed on $Mg^+(CO_2)_n$, where $n = 0$, 1, 2, and 3, using the GAUSSIAN 94 program package.[39] Two gradient-corrected functionals, denoted B3LYP and BP86, were used to compute the geometries, energies, and harmonic vibrational frequencies. Energies were converged to at least 10^{-6} hartrees in the self-consistent field procedures, although the absolute accuracy may be somewhat lower due to numerical integration procedures. The B3LYP functional is a hybrid Hartree−Fock and density functional theory (HF/DFT) method using Becke's three-parameter exchange functional (B3)[40] with the Lee, Yang, and Parr correlation functional (LYP).[41] The BP86 functional uses Becke's 1988 exchange functional (B)[42] and the 1986 correlational correction of Perdew (P86).[43] We employed a triple-ζ basis set with polarization functions, denoted TZP. This basis was constructed from the Huzinage−Dunning[44,45] set of contracted triple-ζ Gaussian functions. Added to this was one set of five d-type polarization functions for each Mg, C, and O atom [$\alpha_d(Mg) = 0.200$, $\alpha_d(C) = 0.654$, and $\alpha_d(O) = 1.211$]. The final contraction scheme for this basis is Mg(13s9p1d/6s5p1d) and C,O(11s6p1d/5s3p1d). Geometries were optimized without any symmetry constraints for each molecular species with each functional using analytic gradient techniques. Residual Cartesian gradients were less than 1.5×10^{-5} hartree/bohr. Stationary points found in optimizations were confirmed as minima by computing the harmonic vibrational frequencies using analytic second derivatives with each functional.

Results and Discussion

Laser vaporization of a magnesium rod in an expansion of pure CO_2 gas produces a distribution of complexes of the form $Mg^+(CO_2)_n$, as described previously.[16] Minor amounts of $MgO^+(CO_2)_n$ clusters are also seen. The distribution of clusters typically extends out to $n = 20$ or so. A similar distribution is obtained in mixed argon/CO_2 expansions with various concentration ratios, except that additional complexes are seen of the form $Mg^+(CO_2)_nAr_m$, for $m = 1-3$.

Carbon dioxide complexes were chosen for these experiments because of the convenient infrared spectroscopy of CO_2. The three vibrations of this linear triatomic are well-known ($\nu_1,\nu_2,\nu_3 = 1333$, 667, 2349 cm^{-1}).[46] The asymmetric stretch and bend are IR-active in the free molecule, but all of these modes may be IR active in metal complexes. However, within the tuning range of our OPO system, we are only able to probe the region of the asymmetric stretch vibration or the region of overtones or combination bands that may occur at higher frequencies.

When these clusters are mass selected and excited near the CO_2 ν_3 asymmetric stretch resonance, the pure CO_2 clusters fragment by losing one or more intact CO_2 molecules. When the mixed clusters are excited, they initially eliminate one or more argon atoms. If the laser power is high enough, argon-containing clusters may go on to lose CO_2 molecules after the argon is lost. Power dependence studies indicate that these multiple fragmentation events are sequential processes. At the lowest laser powers employed, pure CO_2 clusters lose only one molecule and argon-containing clusters lose only one argon atom. This fragmentation behavior is much the same as that which we reported for $Fe^+(CO_2)_n$ and $Fe^+(CO_2)_nAr_m$ clusters.[35] The known and calculated bonding energetics for $Mg^+(CO_2)_n$ clusters in the small size range ($n = 1-3$) suggest that elimination of CO_2 should require at least two photons in these systems. For example, the $Mg^+(CO_2)$ bond energy has been determined previously in our laboratory to be 14.7 kcal/mol ($\sim$5140 cm^{-1}),[16] while this has been calculated to be 16.4 kcal/mol.[24b] The binding energy of $Mg^+(CO_2)_2$ (with respect to the loss of the first ligand) has been calculated at about 11.0 kcal/mol (3850 cm^{-1}). The measured power dependence for these small systems indicates that more than one photon is required to dissociate these systems. The known and calculated bond energy for Mg^+-Ar indicates that elimination of argon is a one photon process. Our group has determined the bond energy to be 1295 cm^{-1},[20a] while it has been calculated at 1041 cm^{-1}.[24g]

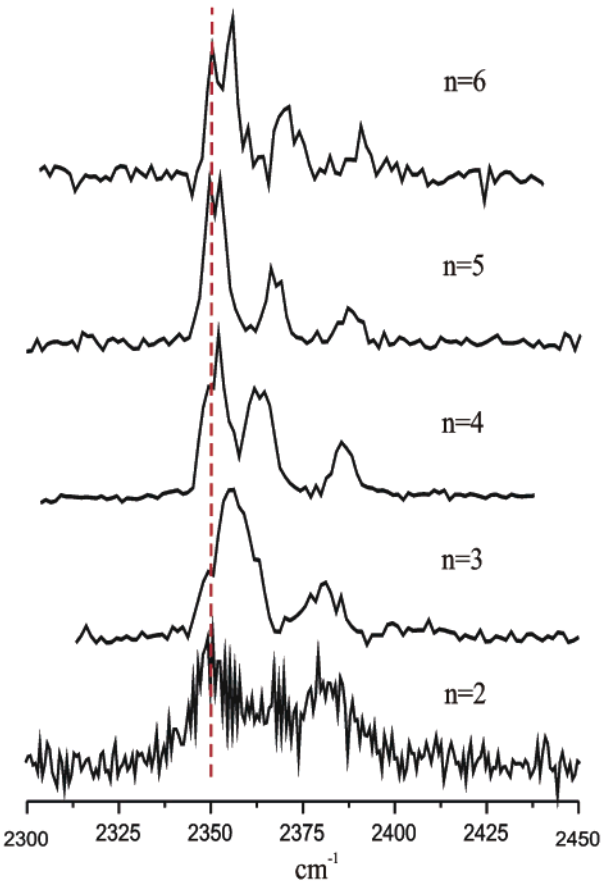

Figure 1. The infrared photodissociation spectroscopy of $Mg^+-(CO_2)_{n=2-6}$ as a function of the laser wavelength from 2310 to 2450 cm^{-1}.

Photodissociation of the mixed complexes is consistent with a one-photon process for argon elimination.

As already observed in our previous study of Fe^+-$(CO_2)_n$ clusters,[35] no fragmentation was obtained for the Mg^+-CO_2 complex, even at the highest laser fluence available. This is consistent with its known bonding energy, which is greater than the one-photon IR excitation energy. Multiphoton absorption and photodissociation could be possible in principle. However, as we have discussed elsewhere,[35] the relatively sparse density of vibrational states in the small complexes is not favorable for a multiphoton absorption process. When the first photon is resonant on a vibrational fundamental, the effects of anharmonicity cause a loss of resonance at the second or higher vibrational levels for that mode. If there are also no other states at the two-photon energy from overtones or combinations of other modes, absorption is difficult except at high laser power when saturation may broaden the resonances. The low state density also limits intramolecular vibrational relaxation (IVR), which is required for the excitation energy to be transferred from the IR chromophore (the asymmetric stretch) to the Mg^+-OCO metal-stretch dissociation coordinate.[35] Thus, it is not too surprising that dissociation of the small complexes would be difficult. As expected, the dissociation of larger complexes is progressively easier, consistent with higher state densities that facilitate multiphoton absorption and provide more rapid IVR rates.

The wavelength dependence of the photodissociation process for $Mg^+(CO_2)_n$ clusters is shown in Figure 1 for the clusters $n = 2-6$ in the wavelength region from 2310 to 2450 cm^{-1}. All of these spectra were recorded at low laser fluence (3 mJ/cm^2) except for the smallest cluster $Mg^+(CO_2)_2$ for which a 25 cm lens was used to compensate for the very low fragmentation yield. Under these experimental conditions, each species undergoes the loss of one CO_2 molecule, and the spectra are obtained by monitoring the intensity of this $n - 1$ fragment channel versus the wavelength of the infrared laser. Recognizable vibrational bands are obtained for all clusters (except the $n = 1$ species) near the position of the asymmetric stretch in the free CO_2 molecule.

For all clusters, the majority of the structure observed lies to the blue of the transition for the free CO_2 molecule (shown in Figure 1 as a vertical dotted line). $Mg^+(CO_2)_2$ has three overlapping bands centered at 2351, 2368, and 2380 $\pm$ 2 cm^{-1}, with a bandwidth of 12 $\pm$ 2 cm^{-1}. As shown, the signal is quite weak for this spectrum. For $Mg^+(CO_2)_3$ the signal is much better, and two bands are observed at 2356 and 2382 $\pm$ 2 cm^{-1}. The first of these is quite broad, with a line width of about 16 cm^{-1}, and the shoulders on both sides could indicate that there are unresolved or overlapping transitions. The second resonance is less intense but somewhat narrower (8 cm^{-1}). For the larger clusters with four, five, and six CO_2 molecules, similar spectra consisting of a set of three bands with approximately the same width (7 $\pm$ 2 cm^{-1}) are obtained. The two most blue shifted transitions at 2363 and 2385 $\pm$1 cm^{-1} for $Mg^+(CO_2)_4$ are slightly more blue shifted upon solvation, occurring at 2368 and 2388 $\pm$1 cm^{-1} for $Mg^+(CO_2)_6$. In each of the $n = 4$, 5, and 6 spectra, the lower energy band exhibits a splitting that gets progressively larger. For $Mg^+(CO_2)_4$, this appears as a shoulder to the red, which evolves into two distinct features for $Mg^+(CO_2)_6$ at 2348 and 2353 $\pm$1 cm^{-1}. However, the position of these two transitions does not change to a great degree with cluster size (within 1 cm^{-1}), but rather the line width gets smaller making the splitting appear greater. The bandwidth could be narrower for larger clusters because they dissociate more easily. The binding energy of CO_2 molecules is expected to decrease as the first solvation shell is completed and fewer infrared photons are required to dissociate the complex, yielding a narrower line width.

The width and congestion in these spectra are very similar to those we have seen previously in the spectra of the corresponding $Fe^+(CO_2)_n$ complexes.[35] The line widths and structure are believed to arise from a number of factors including the possible presence of isomeric structures and the role of power broadening and saturation. The latter is especially likely for the $n = 2$ complex which requires extremely high laser power to measure any dissociation. In previous work on halide anion-molecular clusters,[47] the broadening in similar IR photodissociation spectra was attributed to warm clusters that were fluxional in structure. As a result of this, the IR spectra were broadened because absorption from different structural configurations contributed to the spectrum. However, although we cannot exclude this completely, we do not believe this explanation is appropriate for the clusters under study here. Our laser vaporization cluster source is quite different from the sources used to make anion clusters in other labs. The anion sources use electron impact on clusters that have already undergone supersonic expansion, and then evaporative cooling takes place during and immediately after cluster growth. In our source, ion complexes form in the laser vaporization plasma and then undergo supersonic expansion *after* cluster growth. We have measured the temperature of mono-ligand clusters via rotationally resolved electronic spectroscopy, and find temperatures in the 3−20 K region.[18,19] Although we cannot guarantee that all the larger clusters are cooled completely by this expansion, it is unlikely that the small clusters studied here would have

temperatures very different from the mono-ligand species that we have characterized before. Our photodissociation efficiencies for different clusters also suggest that they are cold. We see extremely low photodissociation cross sections here for the $n = 2$ complex and this improves with cluster size. If $n = 2$ was warm enough to be fluxional in structure, its photodissociation should be easier because of that internal energy. As a final note, these cation clusters are a good deal more strongly bound than the previously studied anions. The charge in metal cation clusters is more localized because of the differences in ionization energies between the metal and CO_2, as opposed to anions clusters where electron affinity differences between cluster components are not so great. Consequently, the cation complexes are expected to have more rigid structures, especially in the small cluster sizes when ligands are attached to the metal. The simplest picture of our clusters therefore, is that they are relatively cold internally and have rather rigid structures. The broad lines seen for species such as $n = 2$ are likely caused by power broadening, since dissociation can only be observed at high laser power.

As cluster size increases, the number and kind of infrared oscillators increases. As we have described for $Fe^+(CO_2)_n$ complexes,[35] the absorption intensity to the blue of the free CO_2 resonance is understandable if the CO_2 ligands bind to the Mg^+ in an end-on configuration. Such a configuration is expected for a charge−quadrupole electrostatic interaction, and it has also been predicted for these complexes by theory.[24b] In the case of the $n = 1$ complex, our previous electronic spectroscopy experiments confirmed that the complex has such an overall $Mg^+-O=C=O$ linear configuration.[16] In this structure, the CO_2 asymmetric stretch vibration is shifted to higher frequency because the molecule experiences increased repulsive interaction on the inside potential wall due to the presence of the metal ion. Depending on the structure of the complex, one or more IR active vibrational bands are expected when multiple ligands bind to the metal ion, and this explains the presence of more than one blue-shifted band in the larger clusters.

It is also possible to understand the bands that occur near the position of the free CO_2 resonance at 2349 cm^{-1}. Absorption here is expected if there are CO_2 ligands in the cluster that are not attached directly to the metal. As we have discussed before,[35] the asymmetric stretch in pure CO_2 clusters (those without metal) shifts by no more than 1−2 cm^{-1} from the free monomer resonance.[48−50] Therefore, CO_2 molecules in these metal ion complexes that are bound only to other CO_2 molecules (i.e., on the surface of the cluster) should also have resonances essentially at the same value as the free CO_2 monomer. The $n = 2$ spectrum is broadened as noted above so that it covers the region around the free molecule frequency and to higher frequency. The $n = 3$ spectrum begins to be more structured, with a small shoulder in this region, but by the $n = 4-6$ clusters there is a clear multiplet peak here. In the small clusters, this feature is likely associated with isomeric clusters that have at least one surface-bound molecule. Although the density of these isomeric structures is not expected to be great, their photodissociation yield should be high because of the relatively weak bonding. The CO_2 dimer bond energy is about 500 cm^{-1},[51] and this is much less than the Mg^+-CO_2 binding energy near 5000 cm^{-1}.[16] Because of these energetic differences, the CO_2 ligands in the small clusters are nearly all expected to be attached to the metal in their minimum energy structures. However, the larger clusters (e.g., $n = 5$ and 6) may have one or more external ligands, and the free-CO_2 band does indeed appear more clearly here.

When such broad spectra are measured in photodissociation spectroscopy, it is often desirable to enhance the photodissociation yield and increase the quality of spectra via the so-called rare gas "tagging" method.[47,52,53] We have described our implementation of this method in our studies of $Fe^+(CO_2)_n$ clusters.[35] To accomplish this here, we make mixed complexes containing both CO_2 and argon bound to Mg^+. The binding energy of Mg^+Ar is 1295 cm^{-1},[20,21] which is considerably less than that of Mg^+CO_2 (5140 cm^{-1}).[16] Therefore, IR-excited clusters containing both argon and CO_2 are expected to fragment by the loss of argon if energy flow (IVR) is efficient throughout the cluster, and this is what we observe. The efficiency of this process should be high, since one IR photon near the CO_2 asymmetric stretch has almost twice the amount of energy needed to break the Mg^+-Ar bond. Argon also adds low-frequency vibrational state density to the clusters, which enhances the rate of IVR and therefore the rate of dissociation. In previous examples of cluster IR spectroscopy, the action spectra measured by elimination of such a rare gas tag resemble those of the untagged clusters in line position, but the line width is narrower and the efficiency of dissociation is greater.[35,47] We therefore have employed this methodology here. Interestingly, all the $Mg^+(CO_2)_nAr$ clusters do dissociate efficiently by losing argon, including the $n = 1$ species that could not be dissociated before.

Figure 2 shows the effect of argon tagging on the $Mg^+(CO_2)_2$ spectrum. The upper trace of the figure shows the spectrum measured without tagging. As indicated in Figure 1, this spectrum is noisy and broadened because of the extreme laser conditions required for dissociation. Three broad bands are apparent. The lower trace shows the dissociation spectrum of $Mg^+(CO_2)_2Ar$ measured in the argon-loss channel. The lower energy band seen in the untagged spectrum near the free-CO_2 resonance is no longer observed, but sharper bands are measured at nearly the same positions of the two higher frequency bands. These sharp features appear at 2368 and 2384 cm^{-1}. The lower energy band seen only in the untagged spectrum could have been caused by an isomer with one CO_2 molecule bound to the other rather than to the metal. This species would have a resonance near the free-CO_2 value, and its band intensity might be artificially enhanced beyond its actual concentration in this photodissociation spectrum because it is much easier to dissociate. In the tagged spectrum, the overall dissociation yield is much greater and unfocused laser excitation is enough to initiate dissociation. Either the other isomer is not formed efficiently when argon is present because argon somehow changes the available binding sites, or the dissociation yield of these isomeric clusters near the free-CO_2 wavelength is not high enough to make the band intensity in this region comparable to the now more intense spectrum.

It is again useful to compare this result to those obtained previously for anion-molecular clusters produced from electron impact cluster sources.[47] In those experiments, argon tagging also produced much simpler vibrational spectra. The mechanism was suggested to be that the argon containing clusters provided a colder subset of species in an otherwise warm cluster distribution, and that these colder complexes had simpler spectra. While this mechanism is indeed reasonable for the anion clusters, we do not believe that it is appropriate here. We have already noted above that our source is different and that clusters *without* argon are already cold.[18,19] The simplest explanation for our complexes is that the argon binding energy is low enough to make one-photon dissociation possible, and this explains the higher dissociation yield and simpler spectra obtained with argon

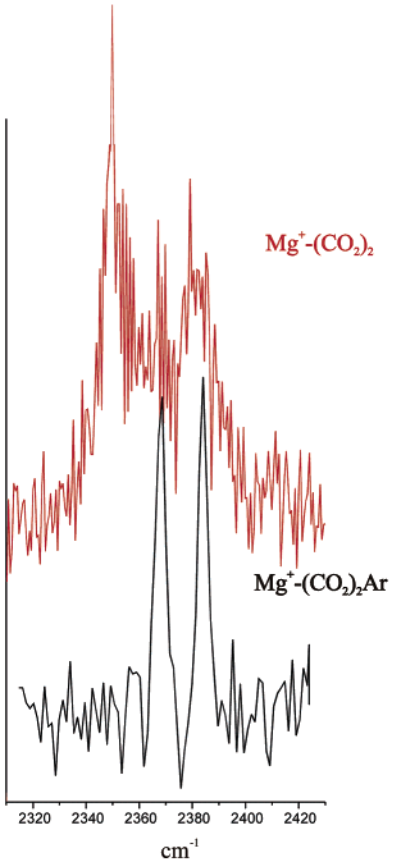

Figure 2. The IR photodissociation spectrum measured for $Mg^+(CO_2)_2$ in the CO_2-loss channel compared to the spectrum of $Mg^+(CO_2)_2Ar$ measured in the Ar-loss channel. As shown, argon tagging eliminates the signal at lower energy, and the bands at higher energy are much sharper.

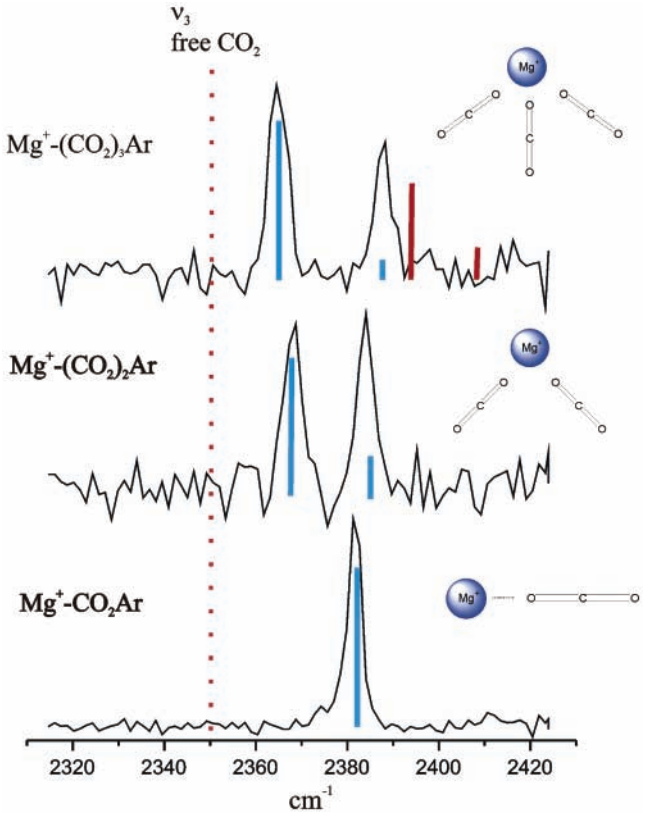

Figure 3. Infrared photodissociation spectroscopy of $Mg^+-(CO_2)_{n=1-3}$-Ar in the asymmetric stretch region of CO_2, measured in the Ar-loss channels. The blue shift for the $n = 1$ complex compared to the free CO_2 molecule is 32 cm^{-1}. For the larger complexes, two bands are observed, corresponding to the in-phase and out-of-phase combinations of the CO_2 asymmetric stretches.

tagging. In both the previous anion systems and the clusters here one must question if the added argon is indeed an innocent bystander from the standpoint of cluster structure. This is a difficult question to answer except to say that spectra do not usually change in their resonance positions when argon is added. Future studies could use tagging with even more weakly binding species such as neon to further test the effects of tagging.

Figure 3 shows the photodissociation spectra of $Mg^+(CO_2)_{1-3}Ar$ as a function of the infrared wavelength from 2310 to 2430 cm^{-1}. The fragmentation channel for each cluster in these spectra is the loss of argon. The dissociation yield is on the order of 10% at low laser fluence (few mJ/cm^2) and increases to 50% using a 25 cm lens. The higher laser power conditions are used for the spectra shown here. For all cluster sizes, strong resonances are found to the blue of the ν_3 transition for the isolated CO_2 molecule (vertical dotted line). For Mg^+-CO_2Ar, only one resonance is observed centered at 2381 ± 1 cm^{-1} while the $Mg^+(CO_2)_2Ar$ complex has two bands at 2368 and 2384 ± 1 cm^{-1} as noted above. $Mg^+(CO_2)_3Ar$ also has a similar two-band spectrum, with resonances at 2364 and 2388 ± 1 cm^{-1}. The line widths observed for these $Mg^+(CO_2)_nAr$ spectra are about 5 cm^{-1}, which is similar to the line widths that we measured previously for $Fe^+(CO_2)_nAr$ complexes.[35] The low internal energy in these complex ions and the weak binding energy of the argon atom provide high fragmentation yields and sharp resonances. Under low infrared fluence conditions, the position and line width of the observed transitions remain unchanged, but the band at 2388 cm^{-1} for $Mg^+(CO_2)_3Ar$ is barely visible. $Mg^+(CO_2)Ar$ undergoes efficient photofragmentation, even at low laser power, which was not the case for $Fe^+(CO_2)Ar$.[35] This is interesting, because the binding energies of both Fe^+ and Mg^+ to CO_2 and Ar are quite similar (about 5000 cm^{-1} for CO_2 and about 1000 cm^{-1} for Ar).[6,9,16,20,24] The corresponding $Mg^+(CO_2)_{1-3}Ar_2$ complexes have also been studied by monitoring the fragment channels associated with the loss of both one and two argon atoms. These spectra are identical to those shown in Figure 3. Therefore, the transitions observed for the argon tagged species are believed to represent the best measurement possible for the position of bands in the absorption spectrum of the corresponding $Mg^+(CO_2)_n$ complexes, and these bands can be used to consider the structures of these clusters.

The qualitative appearance of the spectra for the smaller clusters (i.e., the number of bands seen) can be used to deduce their structures. The $n = 1$ complex was determined previously to have a linear structure,[16] and theory also predicts this.[24] For such a linear structure, only one IR-active vibrational mode is expected in the region of the asymmetric stretch, and only one band is seen here. Therefore, this IR spectrum is completely consistent with the linear structure found in previous measurements. The $n = 2$ complex can have two vibrational modes in the region of the asymmetric stretch derived from in-phase and out-of-phase motions of this type on the two ligands. If the structure is overall linear (i.e., O=C=O−Mg^+−O=C=O), then only the out-of-phase motion is IR-active and only one band is expected in this region. We found this behavior for the corresponding $Fe^+(CO_2)_2$ complex.[35] However, if the structure is bent, then both the in-phase and out-of-phase vibrations are IR-active in much the same way that the symmetric and asymmetric O−H stretches in water are both IR-active. Two

bands are therefore expected in this region, and indeed two bands are observed. This proves that the $Mg^+(CO_2)_2$ complex is bent. Bauschlicher and co-workers actually predicted that the n=2 complex would be bent based on their theoretical calculations.[24b] The rationale for this is the high polarizability of the valence *3s* electron of Mg^+. When a ligand such as CO_2 binds to Mg^+, the linear structure results from the charge−quadrupole interaction, as noted above. However, the negative end of the CO_2 is able to polarize the valence electron of Mg^+, and this results in a lobe of negative charge at a position opposite the first ligand's binding site. When a second CO_2 arrives, it apparently avoids this negative charge region and binds more effectively in a bent configuration. Bauschlicher calculated that the angle between the two CO_2 ligands would be about 88°.[24b] Similar considerations can also be applied to the $n = 3$ complex. The possible vibrational modes near the asymmetric stretch can be constructed from in-phase and out-of-phase combinations of this motion on the three CO_2 ligands. If the structure is trigonal planar, the in-phase combination is not IR-active, but the degenerate (2 + 1) out-of-phase motion is active, and only one vibrational band would be expected. However, if the same kind of valence electron polarization effect causes the structure to be bent, then both kinds of vibrations would be IR-active and two bands would be expected here. The observation of two bands for $Mg^+(CO_2)_3$ is then consistent with a nonplanar structure such as a trigonal pyramid.

To investigate these structural issues more quantitatively, DFT calculations were performed on the $Mg^+(CO_2)_{1-3}$ complexes using both the B3LYP and BP86 functionals. The minimum energy structures derived from these calculations without any symmetry constraints in the optimizations are shown in Figure 4, and the energetics of binding in these configurations are summarized in Table 1. For the 1−1 and 1−2 complexes, the structures found are nearly the same as those reported by Bauschlicher and co-workers.[24b] The 1−3 complex has not been studied previously. In all three complexes, the CO_2 ligand binds with an oxygen toward the metal, as expected for the charge−quadrupole electrostatic interaction. In the $n = 1$ complex, the Mg^+−O bond distance is 2.134 or 2.156 Å for B3LYP or BP86 functionals. Bauschlicher found a slightly shorter value of 2.10 Å.[24b] In the $n = 2$ complex, this bond distance increases to 2.182 or 2.205 Å. As Bauschlicher has discussed previously,[24b] the second ligand approaches from the side resulting in a C_{2v} structure. While Bauschlicher found an O−Mg^+−O angle of 88°, we find an angle of 89.0° or 90.2° with the B3LYP or BP86 functionals, respectively. Closer approach of the ligands to each other is not favored because their quadrupole moments repel each other in the aligned parallel configuration. In the $n = 2$ complex, the Mg^+−OCO angle is not linear, but rather is close to 165° for both functionals. The lowest energy $n = 3$ complex also has all three ligands binding on the same side of the ion (C_{3v} symmetry), due to the same polarization effect discussed above. The Mg^+−O bond distance increases further to 2.216/2.236 Å, and the Mg^+−OCO angle decreases to about 160°, i.e., it is bent more away from the linear configuration. The metal−ligand bond energy for the $n = 1$ complex is (B3LYP) $D_e = 15.8$ and $D_0 = 15.4$ kcal/mol. These compare with the previous value calculated by Bauschlicher of $D_0 = 16.4$ kcal/mol[24b] and our experimental value of $D_0 = 14.7$ kcal/mol.[16] The incremental binding for the $n = 2$ and 3 complexes are $D_0 = 10.8$ and 8.3 kcal/mol, respectively. The second and third ligands are bound more weakly than the first. A similar trend was found by Bauschlicher for the $n = 1$ and 2 complexes.[24b]

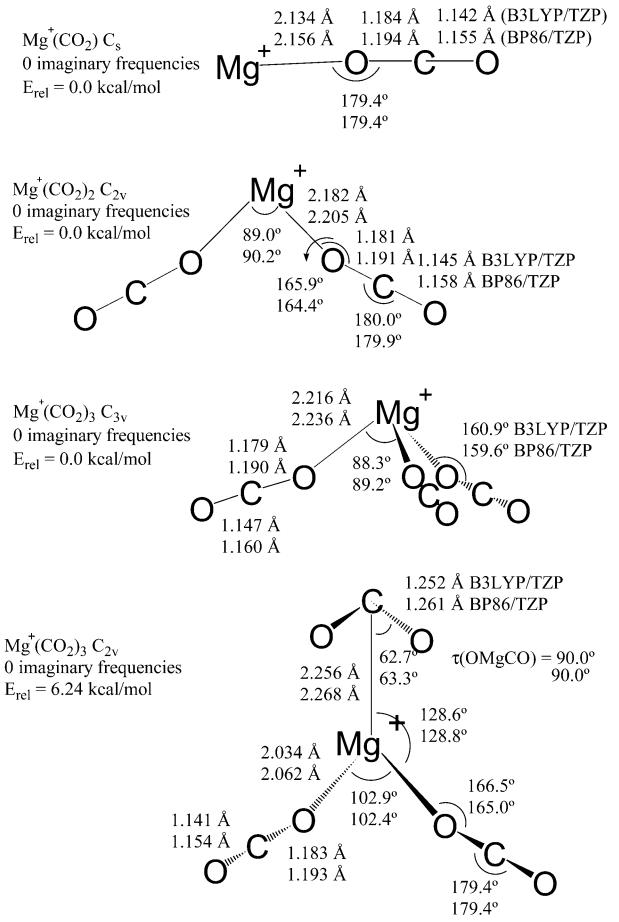

Figure 4. Optimized DFT geometries of Mg^+−$(CO_2)_{n=1-3}$ with structural parameters for the B3LYP and BP86 functionals. Only one structural minimum is found for the $n = 1$ and 2 species, but $n = 3$ has both C_{3v} and C_{2v} isomers.

TABLE 1: Total Electronic Energies of Mg^+, CO_2, $Mg^+(CO_2)$, $Mg^+(CO_2)_2$, and $Mg^+(CO_2)_3$ with a TZP Basis Set

system	B3LYP[a]	D_e (kcal/mol)	BP86[a]	D_e (kcal/mol)
Mg^+	−199.80911		−199.80089	
	(−199.80911)		(−199.80089)	
CO_2	−188.65686		−188.66504	
	(−188.64517)		(−188.65377)	
Mg^+CO_2	−388.49115	15.8	−388.49004	15.1
	(−388.47880)	(15.4)	(−388.47815)	(14.7)
$Mg^+(CO_2)_2$	−577.16616	27.4	−577.17231	25.9
	(−577.14122)	(26.2)	(−577.14849)	(25.1)
$Mg^+(CO_2)_3$ (C_{3v})	−765.83717	36.1	−765.85063	34.3
	(−765.79966)	(34.5)	(−765.81465)	(32.9)
$Mg^+(CO_2)_3$ (C_{2v})	−765.82722	29.8	−765.83761	26.1
	(−765.98979)	(28.4)	(−765.80175)	(24.8)

[a] Energies are in hartrees. Zero-point corrected values are listed in parentheses.

To investigate the possible role of isomeric structures, we have also explored structures for these small systems that have inequivalent CO_2 ligands. For example we explored a configuration for the $n = 2$ complex with one ligand attached to metal in the linear configuration and a second CO_2 bound in a "T" configuration. This "T" binding configuration was also explored for the $n = 1$ complex. In both the $n = 1$ and 2 complexes, such "T" bonded configurations were found not to be local minima. A similar configuration was explored for $n = 3$, and in this case the C_{2v} structure with side-bonded CO_2 is found to

TABLE 2: Theoretical Harmonic Vibrational Frequencies in cm^{-1} of CO_2 and $Mg^+(CO_2)_n$ with a TZP Basis Set[a]

CO_2	B3LYP	BP86	exptl	CO_2	B3LYP	BP86	exptl
ω_1 (Σ_g)	1373 (0.0)	1317 (0.0)	1333	ω_3 (Π_u)	675 (35.4)	641 (25.8)	667
ω_2 (Σ_u)	2410 (681.1)	2349 (555.5)	2349	ω_4 (Π_u)	675 (35.4)	641 (25.8)	667
Mg^+CO_2	B3LYP	BP86	exptl	Mg^+CO_2	B3LYP	BP86	exptl
ω_1 (A′)	2443 (857.0)	2378 (695.9)		ω_4	237 (104.1)	230 (103.0)	
ω_1 (corrected)	2382		2381	ω_5	72 (1.9)	68 (2.1)	
ω_2	1372 (74.2)	1319 (59.3)		ω_6 (A″)	648 (39.6)	612 (31.3)	
ω_3	648 (39.9)	612 (31.3)					
$Mg^+(CO_2)_2$	B3LYP	BP86	exptl	$Mg^+(CO_2)_2$	B3LYP	BP86	exptl
ω_1 (A_1)	2446 (455.0)	2378 (695.9)		ω_9 (B_1)	652 (73.0)	614 (57.6)	
ω_1 (corrected)	2385		2384	ω_{10}	60 (0.4)	48 (0.6)	
ω_2	1373 (27.5)	1317 (16.5)		ω_{11} (B_2)	2428 (1456.4)	2364 (1241.6)	
ω_3	650 (45.5)	610 (29.0)		ω_{11} (corrected)	2367		2368
ω_4	223 (82.70	212 (78.3)		ω_{12}	1370 (78.3)	1315 (59.6)	
ω_5	90 (0.08)	81 (0.05)		ω_{13}	647 (26.4)	609 (24.0)	
ω_6	31 (1.3)	27 (1.2)		ω_{14}	202 (82.7)	195 (84.9)	
ω_7 (A_2)	651 (0.0)	613 (0.0)		ω_{15}	59 (0.06)	54 (0.03)	
ω_8	65 (0.0)	56 (0.0)					
$Mg^+(CO_2)_3$ (C_{3v})	B3LYP	BP86	exptl	$Mg^+(CO_2)_3$ (C_{3v})	B3LYP	BP86	exptl
ω_1	2449 (225.4)	2374 (103.4)		ω_{13}	37 (1.1)	34 (1.1)	
ω_1 (corrected)	2388		2388	ω_{14}	26 (0.4)	22 (0.4)	
ω_2	2425 (1423.8)	2355 (1160.7)		ω_{15} (A″)	2425 (1412.4)	2356 (1142.2)	
ω_2 (corrected)	2364		2364	ω_{15} (corrected)	2364		2364
ω_3	1374 (7.4)	1312 (0.9)		ω_{16}	1371 (49.9)	1311 (31.1)	
ω_4	1371 (50.2)	1311 (30.7)		ω_{17}	654 (52.2)	564 (41.1)	
ω_5	653 (49.9)	564 (42.9)		ω_{18}	649 (1.4)	560 (0.5)	
ω_6	649 (60.3)	556 (37.2)		ω_{19}	646 (10.4)	555 (14.4)	
ω_7	647 (14.2)	555 (12.7)		ω_{20}	191 (58.8)	189 (60.0)	
ω_8	223 (70.1)	215 (60.7)		ω_{21}	87 (0.01)	77 (0.04)	
ω_9	194 (59.8)	192 (60.3)		ω_{22}	62 (0.5)	56 (0.2)	
ω_{10}	99 (0.0)	89 (0.0)		ω_{23}	54 (0.0)	43 (0.0)	
ω_{11}	87 (0.03)	76 (0.1)		ω_{24}	27 (0.4)	24 (0.4)	
ω_{12}	63 (0.7)	58 (0.3)					
$Mg^+(CO_2)_3$ (C_{2v})	B3LYP	BP86	exptl	$Mg^+(CO_2)_3$ (C_{2v})	B3LYP	BP86	exptl
ω_1	2470 (373.0)	2402 (296.7)		ω_{12}	513 (133.0)	482 (108.2)	
ω_1 (corrected)	2409		2388	ω_{13}	411 (98.6)	395 (84.2)	
ω_2	2455 (1441.6)	2389 (1233.2)		ω_{14}	350 (7.9)	330 (7.8)	
ω_2 (corrected)	2394		2364	ω_{15}	323 (66.4)	304 (75.6)	
ω_3	1585 (565.3)	1562 (482.3)		ω_{16}	221 (2.9)	204 (5.4)	
ω_4	1393 (34.5)	1339 (26.1)		ω_{17}	131 (17.9)	118 (16.9)	
ω_5	1390 (112.2)	1336 (92.6)		ω_{18}	108 (1.8)	99 (1.6)	
ω_6	1335 (1.1)	1262 (12.1)		ω_{19}	101 (9.2)	92 (7.7)	
ω_7	834 (4.5)	792 (0.6)		ω_{20}	90 (0.0)	81 (0.0)	
ω_8	647 (78.0)	610 (49.9)		ω_{21}	37 (0.0)	33 (0.0)	
ω_9	646 (82.4)	609 (62.4)		ω_{22}	36 (5.7)	32 (5.0)	
ω_{10}	645 (15.9)	608 (12.3)		ω_{23}	33 (12.0)	30 (11.0)	
ω_{11}	644 (0.0)	608 (0.0)		ω_{24}	28 (0.03)	25 (0.0)	

[a] IR intensities are given in parentheses in km/mol.

be a local minimum lying 6.24 kcal/mol above the C_{3v} structure. As shown in Figure 4, this structure has two end-on CO_2 molecules and the side-bonded ligand is also significantly bent with oxygen atoms closer to the metal. Depending on the temperature and the dynamics of cluster growth, it is therefore conceivable that the $n = 3$ complex could have either one or both of these isomeric structures present in the molecular beam.

Table 2 provides the harmonic vibrational frequencies calculated for these various complexes and the comparison to our experimental values. The IR oscillator strengths calculated appear in parentheses. As expected, the B3LYP harmonic vibrational frequencies overshoot the experimental values. We therefore have calculated the vibrations of the free CO_2 molecule at the same level of theory and we apply a frequency shift based on this result to correct the vibrations in the complexes for the effects of anharmonicity. The "corrected" vibrational predictions for the asymmetric stretch-related modes also appear in Table 2. With the B3LYP functional, the free CO_2 ν_3 mode is calculated at 2410 cm^{-1}, which is 61 cm^{-1} to the blue of the actual transition. All the frequencies calculated for the complexes that involve the asymmetric stretch mode have therefore been reduced by this same amount. The BP86 calculations fall exactly on the experimental value of the free CO_2 asymmetric stretch, and therefore no correction is applied in this coordinate for the complexes. The B3LYP corrected vibrational bands are added to Figure 3 as vertical blue or red bars (see below) with the approximate relative intensities of the calculated vibrations indicated.

As shown in Table 2, and illustrated dramatically in Figure 3, the vibrational band positions predicted via the B3LYP shifted calculations are in remarkable agreement with the experimental values measured with argon tagging. We measure the asymmetric stretch in the $n = 1$ complex at 2381 cm^{-1} while the predicted value for this mode is 2382 cm^{-1}. The out-of-phase

(B_2) and in-phase (A_1) combinations of ν_3 in the $n = 2$ complex are predicted at 2367 and 2385 cm^{-1}, respectively, while our experimental values lie at 2368 and 2384 cm^{-1}. In the $n = 3$ complex, vibrations are calculated for both the C_{2v} and C_{3v} isomeric structures. For the lowest energy C_{3v} structure, the in-phase combination of the asymmetric stretch on the three ligands is calculated at 2388 cm^{-1}, while the out-of-phase combination is at 2364 cm^{-1}. These values for the lowest energy isomer are indicated as blue bars in the figure, and the experiment measures exactly these values. The C_{2v} structure is calculated also to have two allowed vibrational bands in this region, but these are predicted at 2394 and 2409 cm^{-1} (indicated as red bars in the figure). These positions are about 30 and 20 cm^{-1} respectively higher in energy than the bands that we observe. Therefore, our spectral data for the $n = 3$ complex is consistent with the C_{3v} isomer that was predicted to be the most stable, and it finds no evidence for the less stable C_{2v} isomer. Taken as a group, these results indicate that the argon-tagged spectra do indeed represent the positions of the absorption bands for the corresponding pure CO_2 complexes. Likewise, the agreement between these measured spectra and theory also suggest that these complexes have essentially the structures calculated, even though argon is present in some undefined position in the experiment. Apparently the CO_2 ligands bind to the metal more strongly (as expected) and the argon atoms do not perturb these structures significantly enough to change their vibrational spectra.

It is interesting to compare the band intensities measured in Figure 3 to the IR absorption strengths calculated (indicated with blue bars). In the $n = 3$ complex, for example, the band at 2388 cm^{-1} is predicted to have an IR oscillator strength of 225 km/mol, while the 2364 cm^{-1} band is doubly degenerate with a combined intensity of about 2850 km/mol. In the spectrum shown, these bands appear with roughly equal intensity. However, as noted above, there is a much larger difference in these two band intensities when they are measured at low laser power (the 2388 band is then barely detectable). Under the higher power conditions used to obtain the spectra shown in the figure, the 2364 band is almost certainly saturated, and then the two bands have similar intensities. A similar effect probably causes the 2367 and 2385 bands in the $n = 2$ spectrum to appear with similar intensity. Although it might be more desirable in the future to use lower laser powers to get more accurate line intensities, working in this higher power mode of operation ensures that we detect all the IR-active bands possible in these spectra.

The results of these calculations and their striking agreement with the spectra of the argon-tagged complexes also provide some insight into the structures of the un-tagged complexes. As noted above, the spectra shown in Figure 1 all have shoulders ($n = 2-4$ complexes) or actual peaks ($n = 5$ and 6 complexes) occurring at the position of the free CO_2 vibration. These shoulders are clearly not present in the argon tagged spectra, nor is any absorption predicted here in the calculations for the lowest energy structures for these complexes. As noted above, resonances at this position in metal ion$-CO_2$ complexes have been associated with surface-bound ligands, i.e., those not attached to the metal ion. The calculations suggest that such structures do not represent the lowest energy species. They must then represent other less-stable isomers formed in the cluster growth, as discussed above. It is quite surprising that such isomers would be formed because the binding energies for surface CO_2 molecules must be much less than for those attached to the metal ion. However, in Figure 1, the shoulders in question

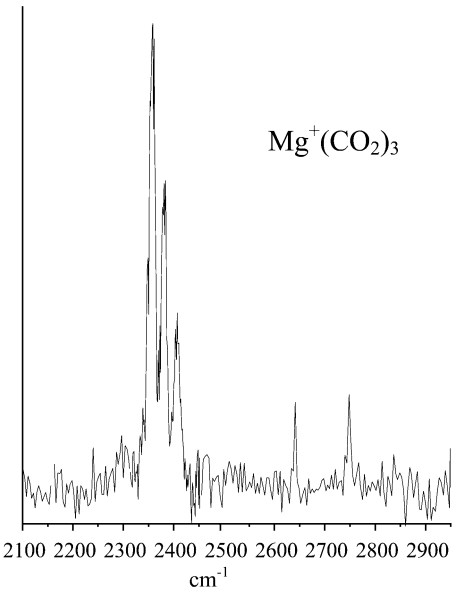

Figure 5. Spectroscopy of Mg^+-$(CO_2)_3$ from 2100 to 2950 cm^{-1} measured with a focused IR laser. The spectrum shows the same bands seen in Figure 1 at 2358 and 2382 cm^{-1}, and there is an additional weaker band near 2407 cm^{-1}. This latter band could be a combination between the asymmetric stretch and a low-frequency bend. Other bands appear to the blue of the ν_3 transition at 2641 and 2748 cm^{-1}. The most likely assignments for these are the combination band ($\nu_1 + 2\nu_2$) and the overtone $2\nu_1$, respectively.

have intensities comparable to the other bands. This could be indicating that these isomers exist in the beam with densities comparable to the other more stable isomers. However, since we measure these spectra by photodissociation rather than absorption, it is not clear that line intensities can be related in a straightforward way with cluster densities. Saturation could affect these band intensities in the same way noted above. Additionally, it could be that these features are artificially enhanced in the pure CO_2 clusters simply because they dissociate easier. A similar effect has been suggested in our study of $Fe^+(CO_2)_n$ clusters.[35] In the argon-tagged species, no evidence is found for these resonances near the free CO_2 position. This could mean that the presence of argon somehow blocks the formation of the minor isomers in the small clusters. On the other hand, it could also be because the argon tagged clusters dissociate quite easily and other isomeric clusters present in low concentration lose their photodissociation advantage and therefore are no longer noticeable on the scale of these spectra. It is clear from this discussion and that in our previous work on $Fe^+(CO_2)_n$ clusters that we need to be especially careful in interpreting band intensities in these spectra measured with photodissociation.

In the IR spectrum of free CO_2, overtone and combination bands can be detected under certain conditions. Figure 5 shows a long scan of $Mg^+(CO_2)_3$ from 2100 to 3000 cm^{-1} to investigate the possibility of such bands in these complexes. This spectrum has been recorded at high laser fluence. The bands seen before in Figure 1 at 2356 and 2382 cm^{-1} are seen again with higher signal levels, and a new spectroscopic feature appears at 2407 $\pm$ 2 cm^{-1}, which is 54 cm^{-1} above the most intense band at 2356. A higher frequency band just above the main features has also been seen in the case of $Fe^+(CO_2)_3$ even at low infrared power.[35] It is believed to be related to a combination band of the asymmetric stretch together with a low-frequency bending mode. As shown in Table 2, bending modes in the range of 50$-$60 cm^{-1} are indeed predicted for this

complex, and so such a combination band makes sense here also. Other new features are seen as bands at 2641 and 2748 cm^{-1}. These lie 285 and 392 cm^{-1} to the blue from the main transition. Table 2 shows that the metal−ligand stretch in this complex is expected near 190 cm^{-1}, and no other bands are predicted between this and the CO_2 ν_2 bending modes at about 640 cm^{-1}. Therefore, it is not likely that these bands come from any combination of the main transition and a lower frequency vibration. However, the free CO_2 molecule exhibits a strong Fermi resonance in the $\nu_1/2\nu_2$ region, the unperturbed frequencies being 1333 and 1334 cm^{-1}, respectively. The splitting induced by this perturbation is about 103 cm^{-1}. It is conceivable that a similar vibrational combination could occur in this complex. The vibrations in the complex corresponding to the monomer ν_1 mode (symmetric stretch) are ν_3, ν_4, and ν_{16}, with frequencies near 1370 cm^{-1}, while the modes ν_{5-7} and ν_{17-19} with frequencies near 650 cm^{-1} correspond to the monomer ν_2 (bend). Combinations of two asymmetric stretch versus one asymmetric stretch plus two bends would lie at about the position of the higher frequency bands. In-phase versus out-of-phase overtones of the symmetric stretch on different ligands might also produce bands here. So indeed, overtone/combination bands can apparently be observed for the $n = 3$ complex, but we were not able to see such bands for other cluster sizes. The $n = 3$ species is optimum for this because the parent ion signal is large and the photodissociation yield is high.

The structural trends documented for the small clusters here ($n = 1-3$) may also provide insight into the growth of larger cluster structures. As discussed above, the free-CO_2 resonance in the small clusters probably comes from minor isomers. The dissociation yields are low and it is difficult to measure these spectra without argon tagging. However, the larger clusters ($n = 4-6$) have much higher dissociation yields and these spectra have higher signal-to-noise ratios. Although band intensities must be viewed with care, the free CO_2 bands are quite prominent here, perhaps indicating the presence of substantial amounts of CO_2 not attached to the metal even in these relatively small cluster sizes. The polarization effect that causes same-side bonding in the small clusters may be causing the clusters in the size range of 4−6 to grow preferentially by adding to the surface of the metal-bound molecules rather than by adding to the electron rich opposite side of the Mg^+. If this pattern of cluster growth continues, larger species may resemble CO_2 clusters with a metal ion imbedded in the surface rather than a metal ion with solvation layers assembled around it. However, if metal−CO_2 clusters behave in the way proposed for various metal-water clusters,[10,13,31] then charge separation ($Mg^+ \rightarrow Mg^{2+} + e^-$) may occur within some larger cluster sizes, and then the polarization effect of the valence electron would be changed or eliminated and a more solvated interior metal dication may be formed. At present we are limited by signal levels and dissociation lifetimes and cannot study the larger clusters. However, instrument modifications are planned to overcome these difficulties, and future measurements may be possible on much larger clusters to address these issues.

Conclusions

Infrared photodissociation spectroscopy is reported for mass-selected $Mg^+(CO_2)_n$ and $Mg^+(CO_2)_nAr$ clusters in the region of the CO_2 asymmetric stretch vibration. The pure CO_2 clusters dissociate by losing CO_2 molecules, while the mixed clusters lose argon. The dissociation yield for both kinds of clusters has resonances near the asymmetric stretch vibration in the free CO_2 molecule. In the pure CO_2 clusters, these resonances are broad and require high laser powers to be detected. Dissociation yields are higher in the argon tagged clusters, and the resonances consist of a few sharp bands for each cluster size. The majority of the resonant structure occurs to higher frequency than the asymmetric stretch in the free CO_2 molecule, consistent with end-on binding of the ligand to the metal ion. This configuration is expected for the charge−quadrupole electrostatic interaction. Weak shoulders in the small clusters and distinct bands in the larger clusters are found exactly at the resonance of the free CO_2 molecule. These are associated with isomeric structures having surface-bound CO_2 molecules. Density functional calculations are carried out on the $Mg^+(CO_2)_n$ clusters for n=1−3. These calculations find structures with the ligands binding preferentially on the same side of the metal ion. The vibrational bands predicted for these structures are in excellent agreement with those measured, confirming the proposed structures. The occurrence of surface-bound CO_2 resonances at small cluster sizes ($n = 4-7$) suggests that additional CO_2 clustering may take place asymmetrically on the same side of the metal ion.

Acknowledgment. We gratefully acknowledge support for this work from the Air Force Office of Scientific Research (Grant F49620-00-1-0118) and the National Science Foundation (Duncan Grant CHE-9983580 and Schaefer Grant CHE-0136186).

References and Notes

(1) Russell, D. H., Ed. *Gas-Phase Inorganic Chemistry*; Plenum: New York, 1989.

(2) Freiser, B. S., Ed. *Organometallic Ion Chemistry*; Kluwer: Dordrecht, 1996.

(3) Duncan, M. A., Ed. *Advances in Metal & Semiconductor Clusters*; Elsevier Science: Amsterdam, 2001; Vol. 5.

(4) Leary, J. A.; Armentrout, P. B., Eds. *Gas-Phase Metal Ion Chemistry*, a special issue of *Int. J. Mass Spectrom.* **2001**, *204*, 1.

(5) Kebarle, P. *Annu. Rev. Phys. Chem.* **1977**, *28*, 445.

(6) Tjelta, B. L.; Armentrout, P. B. *J. Phys. Chem. A* **1997**, *101*, 2064. (b) Armentrout, P. B.; Baer, T. *J. Phys. Chem.* **1996**, *100*, 12866. (c) Sievers, M. R.; Jarvis, L. M.; Armentrout, P. B. *J. Am. Chem. Soc.* **1998**, *120*, 1891. (d) Dalleska, N. F.; Honma, K.; Sunderlin, L. S.; Armentrout, P. B. *J. Am. Chem. Soc.* **1994**, *116*, 3519. (e) Meyer, F.; Khan, F. A.; Armentrout, P. B. *J. Am. Chem. Soc.* **1995**, *117*, 9740. (f) Armentrout, P. B.; Hales, D. A.; Lian, L. *Adv. Met. Semicond. Clusters* **1994**, *2*, 1. (g) Rogers, M. T.; Armentrout, P. B. *Mass Spectrom. Rev.* **2000**, *19*, 215. (h) Tjelta, B. L.; Walter, D.; Armentrout, P. B. *Int. J. Mass Spectrom.* **2001**, *204*, 7.

(7) Weis, P.; Kemper, P. R.; Bowers, M. T. *J. Phys. Chem. A* **1997**, *101*, 8207. (b) Zhang, Q.; Kemper, P. R.; Bowers, M. T. *Int. J. Mass. Spectrom.* **2001**, *210−211*, 265. (c) Zhang, Q.; Kemper, P. R.; Shin, S. K.; Bowers, M. T. *Int. J. Mass. Spectrom.* **2001**, *204*, 281. (d) Kemper, P. R.; Weiss, P.; Bowers, M. T.; Maitre, P. *J. Am. Chem. Soc.* **1998**, *120*, 13494. (e) Weis, P.; Kemper, P. R.; Bowers, M. T. *J. Phys. Chem. A* **1997,** *101*, 2809.

(8) Walker, N. R.; Firth, S.; Stace, A. J. *Chem. Phys. Lett.* **1998**, *292*, 125. (b) Stace, A. J.; Walker, N. R.; Firth, S. *J. Am. Chem. Soc.* **1997**, *119*, 10239. (c) Stace, A. J. *Adv. Met. Semicond. Clusters* **2001**, *5*, 121.

(9) Dunbar, R. C.; Klippenstein, S. J.; Hrusak, J.; Stöckigt, D.; Schwartz, H. *J. Am. Chem. Soc.* **1996**, *118*, 5277. (b) Ho, Y. P.; Yang, Y. C.; Klippenstein, S. J.; Dunbar, R. C. *J. Phys. Chem. A* **1997**, *101*, 3338.

(10) Beyer, M.; Berg, C.; Görlitzer, H. W.; Schindler, T.; Achatz, U.; Albert, G.; Niedner-Schatteburg, G.; Bondybey, V. E. *J. Am. Chem. Soc.* **1996**, *118*, 7386. (b) Beyer, M.; Achatz, U.; Berg, C.; Joos, S.; Niedner-Schatteburg, G.; Bondybey, V. E. *J. Phys. Chem. A* **1999**, *103*, 671. (c) Bondybey, V. E.; Beyer, M.; Achatz, U.; Fox, B.; Niedner-Schatteburg, G. *Adv. Met. Semicond. Clusters* **2001**, *5*, 295.

(11) Lessen, D. E.; Ascher, R. L.; Brucat, P. J. *Adv. Met. Semicond. Clusters* **1993**, 1, 267.

(12) Asher, R. L.; Bellert, D.; Buthelezi, T.; Weerasekera, G.; Brucat, P. J. *Chem. Phys. Lett.* **1994**, *228*, 390. (b) Asher, R. L.; Bellert, D.; Buthelezi, T.; Brucat, P. J. *Chem. Phys. Lett.* **1994**, *227*, 623.

(13) Fuke, K.; Hasimoto, K.; Takasu, R. *Adv. Met. Semicond. Clusters* **2001**, 5, 1.

(14) Kleiber, P. D. *Adv. Met. Semicond. Clusters* **2001**, 5, 267.

(15) Velegrakis, M. *Adv. Met. Semicond. Clusters* **2001**, 5, 227.

(16) Yeh, C. S.; Willey, K. F.; Robbins, D. L.; Duncan, M. A. *J. Phys. Chem.* **1992**, *96*, 7833. (b) Willey, K. F.; Yeh, C. S.; Robbins, D. L.; Pilgrim, J. S.; Duncan, M. A. *J. Chem. Phys.* **1993**, *98*, 1867.

(17) Scurlock, C. T.; Pullins, S. H.; Duncan, M. A. *J. Chem. Phys.* **1996**, *105*, 3579.

(18) Yeh, C. S.; Pilgrim, J. S.; Robbins, D. L.; Willey, K. F.; Duncan, M. A. *Int. Rev. Phys. Chem.* **1994**, *13*, 231. (b) Duncan, M. A. *Annu. Rev. Phys. Chem.* **1997**, *48*, 69.

(19) Scurlock, C. T.; Pullins, S. H.; Reddic, J. E.; Duncan, M. A. *J. Chem. Phys.* **1996**, *104*, 4591. (b) Pullins, S. H.; Reddic, J. E.; France, M. R.; Duncan, M. A. *J. Chem. Phys.* **1998**, *108*, 2725. (c) France, M. R.; Pullins, S. H.; Duncan, M. A. *J. Chem. Phys.* **1998**, *109*, 8842.

(20) Pilgrim, J. S.; Berry, K. R.; Duncan, M. A. *J. Chem. Phys.* **1994**, *100*, 7945. (b) Reddic, J. E.; Duncan, M. A. *J. Chem. Phys.* **1999**, *110*, 9948. (c) Pullins, S. H.; Scurlock, C. T.; Reddic, J. E.; Duncan, M. A. *J. Chem. Phys.* **1996**, *104*, 7518.

(21) Duncan, M. A. *Int. J. Mass Spectrom.* **2000**, *200*, 545.

(22) Posey, L. A. *Adv. Met. Semicond. Clusters* **2001,** *5*, 145.

(23) Faherty, K. P.; Thompson, C. J.; Aguirre, F.; Michne, J.; Metz, R. B. *J. Phys. Chem. A* **2001**, *105*, 10054.

(24) Bauschlicher, C. W.; Sodupe, M.; Partridge, H. *J. Chem. Phys.* **1992**, *96*, 4453. (b) Sodupe, M.; Bauschlicher, C. W.; Partridge, H. *Chem. Phys. Lett.* **1992**, *192*, 185. (c) Partridge, H.; Bauschlicher, C. W. *Chem. Phys. Lett.* **1992**, *195*, 494. (d) Sodupe, M.; Bauschlicher, C. W. *Chem. Phys.* **1994**, *185*, 163. (e) Maitre, P.; Bauschlicher, C. W., *Chem. Phys. Lett.* **1994**, 225, 467. (f) Sodupe, M.; Branchadell, V.; Rosi, M.; Bauschlicher, C. W. *J. Phys. Chem. A* **1997**, *101*, 7854. (g) Bauschlicher, C. W.; Partridge, H. *Chem. Phys. Lett.* **1995**, *239*, 241.

(25) Ma, J. C.; Dougherty, D. A. *Chem. Rev.* **1997**, *97*, 1303. (b) Dougherty, D. A. *Science* **1996**, *271*, 163.

(26) Caldwell, J. W.; Kollman, P. A. *J. Am. Chem. Soc.* **1995**, *117*, 4177.

(27) Feller, D.; Glendening, E. D.; de Jong, W. A. *J. Chem. Phys.* **1999**, *110*, 1475.

(28) Yang, C. N.; Klippenstein, S. J. *J. Phys. Chem.* **1999**, *103*, 1094. (b) Klippenstein, S. J.; Yang, C. N. *Int. J. Mass Spectrom.* **2000**, *201*, 253.

(29) Chaquin, P.; Costa, D.; Lepetit, C.; Che, M. *J. Phys. Chem. A* **2001**, *105*, 4541.

(30) Pandey, R.; Rao, B. K.; Jena, P.; Alvarez Blanco, M. *J. Am. Chem. Soc.* **2001**, *123*, 3799.

(31) Watanabe, H.; Iwata, S. *J. Phys. Chem.* **1996**, *100*, 3377. (b) Watanabe, H.; Iwata, S., *J. Phys. Chem. A* **1997** *101*, 487. (c) Fuke, K.; Hashimoto, K.; Iwata, S. *Adv. Chem. Phys.* **1999**, *110*, 431.

(32) Cabarcos, O. M.; Weinheimer, C. J.; Lisy, J. M. *J. Chem. Phys.* **1998**, *108*, 5151. (b) Cabarcos, O. M.; Weinheimer, C. J.; Lisy, J. M. *J. Chem. Phys.* **1999**, *110*, 8429. (c) Lisy, J. M. *Int. Rev. Phys. Chem.* **1997**, *16*, 267. (d) Lisy, J. M. *Cluster Ions* **1993**, 217. Ng, C.; Baer, T.; Powis, I., Editors, Wiley: Chichester, UK. (e) Weinheimer, C. J.; Lisy, J. M. *J. Chem. Phys*. **1996**, *105*, 2938.

(33) Agreiter, J. K.; Knight, A. M.; Duncan, M. A. *Chem. Phys. Lett.* **1999**, *313*, 162.

(34) Yang, D. S.; Miyawaki, J. *Chem. Phys. Lett.* **1999**, *313*, 514. (b) Rothschopf, G. K.; Perkins, J. S.; Li, S.; Yang, D. S. *J. Phys. Chem. A* **2000**, *104*, 8178.

(35) Gregoire, G.; Velasquez, J.; Duncan, M. A. *Chem. Phys. Lett.* **2002**, *349*, 451. (b) Gregoire, G.; Duncan, M. A. *J. Chem. Phys.* **2002**, *117*, 2120.

(36) van Heijnsbergen, D.; von Helden, G.; Meijer, G.; Maitre, P.; Duncan, M. A. *J. Am. Chem. Soc*. **2002**, *124*, 1562.

(37) Velasquez, J.; Kirschner, K. N.; Reddic, J. E.; Duncan, M. A. *Chem. Phys. Lett.* **2001**, *343*, 613.

(38) Nakamoto, K. *Infrared and Raman Spectra of Inorganic and Coordination Compounds*, 5th ed.; John Wiley: New York, 1997; Parts A and B.

(39) Frisch, M. J.; Trucks, G. W.; Schlegel, H. B.; Gill, P. M. W.; Johnson, B. G.; Robb, M. A.; Cheeseman, J. R.; Keith, T.; Petersson, G. A.; Montgomery, J. A.; Raghavachari, K.; Al-Laham, M. A.; Zakrzewski, V. G.; Ortiz, J. V.; Foresman, J. B.; Cioslowski, J.; Stefanov, B. B.; Nanayakkhara, A.; Challacombe, M.; Peng, C. Y.; Ayala, P. Y.; Chen, W.; Wong, M. W.; Andres, J. L.; Replogle, E. S.; Gomperts, R.; Martin, R. L.; Fox, D. J.; Binkley, J. S.; Defrees, D. J.; Baker, J.; Stewart, J. P.; Head-Gordon, M.; Gonzalez, C.; Pople, J. A. GAUSSIAN 94, revision C.3; Gaussian, Inc.: Pittsburgh, PA, 1995.

(40) Becke, A. D. *J. Chem. Phys.* **1993**, *98*, 5648.

(41) Lee, C.; Yang, W.; Parr, R. G. *Phys. Rev. B* **1988**, *37*, 785.

(42) Becke, A. D. *Phys. Rev. A* **1988**, *98*, 3098.

(43) Perdew, J. P. *Phys. Rev. B* **1986**, *33*, 7046.

(44) Huzinaga, S. *J. Chem. Phys.* **1965**, *42*, 1293.

(45) Dunning, T. H. *J. Chem. Phys.* **1970**, *53*, 2823.

(46) Shimanouchi, T. *Molecular Vibrational Frequencies*, 69th ed.; Chemistry WebBook, NIST Standard Reference Database (http://webbook.nist.gov); 2001.

(47) Ayotte, P.; Weddle, G. H.; Kim, J.; Johnson, M. A. *J. Am. Chem. Soc.* **1998**, *120*, 1236. (b) Ayotte, P.; Weddle, G. H.; Kim, J.; Johnson, M. A. *Chem. Phys.* **1998**, *239*, 253.

(48) Walsh, M. A.; England, T. H.; Dyke, T. R.; Howard, B. J. *Chem. Phys. Lett.* **1985**, *120*, 313.

(49) Weida, M. J.; Sperhac, J. M.; Nesbitt, D. *J. Chem. Phys.* **1995**, *103*, 7685.

(50) Jucks, K. W.; Huang, Z. S.; Miller, R. E.; Fraser, G. T.; Pine, A. S.; Lafferty, W. J. *J. Chem. Phys.* **1988**, *88*, 2185.

(51) Bukowski, R.; Sadlej, J.; Jeziorski, B.; Jankowski, P.; Szalewicz, K.; Kucharski, S. A.; Williams, H. L.; Rice, B. M. *J. Chem. Phys.* **1999**, *110*, 3785.

(52) Knickelbein, M. B.; Menezes, W. J. C. *Phys. Rev. Lett.* **1992**, *69*, 1046. (b) Menezes, W. J. C.; Knickelbein, M. B. *J. Chem. Phys.* **1993**, *98*, 1856.

(53) Pino, T.; Boudin, N.; Brechignac, P. *J. Chem. Phys.* **1999**, *111*, 7337.